

and 55 in the N-terminal is involved in the basolateral targeting of mUT-A3, probably via an interaction with the AP1- μ 1B subunit.

Stewart *et al.* (2004), *Am.J.Physiol.*, **286**, F979-87

Cooper and Collins, (2006), *FASEB J.*, **20**, A1219

Folsch *et al.* (1999), *Cell* **99**, 189-198.

The financial support of Kidney Research UK is gratefully acknowledged. The LLC-PK1- μ 1B cell line was a generous gift from Prof Ira Mellman.

Authors have confirmed where relevant, that experiments on animals and man were conducted in accordance with national and/or local ethical requirements.

C41

TASK-3 potassium channels: gating at the cytoplasmic mouth of the channel

P.R. Stanfield¹, I. Ashmole¹, P.J. Stansfeld² and M.J. Sutcliffe³

¹Biological Sciences, University of Warwick, Coventry, UK,

²Biochemistry, University of Oxford, Oxford, UK and ³Manchester Interdisciplinary Biocentre, University of Manchester, Manchester, UK

We have used patch- and two electrode voltage-clamp recording, site directed mutagenesis and molecular model building to ask whether the tandem pore potassium channel TASK-3 is gated at the 'helix bundle crossing'.

Although tandem pore channels are described as constitutively open, the P(open) of wild type TASK-3 channels, heterologously expressed in CHO cells, was only 0.023 ± 0.0004 (mean \pm sem, n=6) at -80mV (140mM-K). P(open) increased with depolarisation, but with a low gating charge ($z'=0.16$). We have used this voltage dependence to examine effects of mutations on gating.

Replacement with threonine of an alanine residue, A237, close to the cytoplasmic end of membrane helix M4, raised P(open) to 0.205 ± 0.031 (n=3) in the same conditions. The voltage dependence of P(open) is shifted to more negative potentials without change in gating charge. The shift gives an energy difference of ~ 1.2 kcal/mol, consistent with the mutant channel being held open by a H-bond (or bonds). Contrary to our previous report, we can find no change in the response of A237T to acidification (measured in channels expressed in *Xenopus* oocytes) (Ashmole *et al.*, 2005). Gating in response to acidification occurs at the selectivity filter (Yuill *et al.*, 2007).

Modelling TASK-1 (which has strong identity with TASK-3) using KvAP (Jiang *et al.*, 2003) as template suggests a H-bond between Thr in position 237 and Asn133, at the cytoplasmic end of M2. However, N133A also has a raised P(open), as does the dual mutant N133A/A237T. Neither mutant form of the channel has an altered response to acidification.

Gating at the bundle crossing of helices M2 and M4 is expected to occur around hinge glycines. Such residues are conserved through the tandem pore family, in TASK-3 at positions 117 (M2) and 231 (M4). In G117A and G231A; P(open) is reduced

to 0.0021 ± 0.0003 (n=3) and 0.0039 ± 0.0013 (n=4) (respectively). The voltage dependence is shifted positive, again without change in gating charge. In spite of a low P(open), macroscopic currents can be recorded from G117A and G231A (oocyte expression). The pH-sensitivity of these currents is again unaltered from wild type.

Voltage dependence is weak and its physiological importance is uncertain. But this voltage dependence appears to involve gating by movements of M2 and M4 similar to those found in other potassium channels. It is likely that modulation of TASK-3 by hormones, neurotransmitters and inhalational anaesthetics (Kim, 2005) occurs by gating at this part of the channel.

Ashmole *et al.* (2005) *J Physiol* 565P PC90

Jiang *et al.* (2003) *Nature* 423:33-41

Kim (2005) *Curr Pharm Des* 11:2717-2735

Yuill *et al.* (2007) *Pfluegers Arch* 455:333-348

We thank the Wellcome Trust for support

Authors have confirmed where relevant, that experiments on animals and man were conducted in accordance with national and/or local ethical requirements.

C42

cAMP-initiated but PKA-independent regulation of vascular ATP-sensitive K⁺ channels: The role of exchange proteins directly activated by cAMP

G.I. Purves¹, T. Kamishima², L.M. Davies¹, J.M. Quayle² and C. Dart¹

¹Biological Sciences, University of Liverpool, Liverpool, UK and

²Department of Human Anatomy and Cell Biology, University of Liverpool, Liverpool, UK

The exchange proteins directly activated by cyclic AMP (Epac or cAMP-GEF) are a family of cAMP-regulated guanine nucleotide exchange factors (GEF) [1]. Binding of cAMP to Epac activates the GEF activity thus stimulating the exchange of GTP for GDP on the monomeric G proteins Rap1/2 [1]. The discovery of the Epac proteins (Epac1/2) has raised the possibility of novel signalling pathways for cAMP that are independent of its traditional target, protein kinase A (PKA). It has previously been reported using yeast two-hybrid screening that Epac interacts with sulphonylurea receptors (SUR) [2], the regulatory subunits of ATP-sensitive potassium (K_{ATP}) channels. This suggests that Epac may play a role in the regulation of K_{ATP} channel activity. Indeed, we found that antibodies directed against Epac1 co-immunoprecipitate SUR2B, the dominant SUR subtype found in vascular smooth muscle, from rat aortic homogenates. Also, using the Epac-specific cAMP analogue 8-pCPT-2'-O-Me-cAMP at concentrations that activate Epac but not PKA, we show cAMP-mediated but PKA-independent modulation of vascular K_{ATP} channels. Application of 8-pCPT-2'-O-Me-cAMP (5 μ M) caused a 41.6 ± 4.7 % inhibition (mean \pm SEM; n = 7) of pinacidil-evoked whole-cell K_{ATP} currents recorded in isolated rat aortic

smooth muscle cells. Consistent with the idea that Epac mediates some of its effects by inducing a rise in intracellular Ca^{2+} [3], we found that the activation of Epac via application of 8-pCPT-2'-O-Me-cAMP (5 μM) caused a transient 171.0 ± 18.0 nM ($n = 5$) increase in intracellular Ca^{2+} in Fura-2-loaded rat aortic smooth muscle myocytes. Inclusion of the Ca^{2+} chelator BAPTA (20 μM) in the pipette-filling solution significantly reduced the ability of 8-pCPT-2'-O-Me-cAMP (5 μM) to inhibit whole-cell K_{ATP} currents (inhibition $8.7 \pm 4.4\%$; $n = 4$; $p < 0.001$; student's t-test). Preincubation with cyclosporin A (10 μM) and ascomycin (5 μM), inhibitors of the Ca^{2+} -sensitive protein phosphatase 2B (PP-2B, calcineurin), also significantly reduced the ability of 8-pCPT-2'-O-Me-cAMP to inhibit whole-cell K_{ATP} currents (inhibition $10.8 \pm 2.8\%$; $n = 9$; $p < 0.001$; student's t-test and $7.3 \pm 1.6\%$; $n = 8$; $p < 0.001$; student's t-test, respectively). These findings suggest cAMP-mediated activation of Epac inhibits aortic K_{ATP} channels via a Ca^{2+} -dependent mechanism involving the activation of calcineurin, and highlight a potentially important role for Epac in regulating vascular tone.

Bos JL (2006). *Trends in Biochemical Sciences* **31**: 680-686.

Ozaki N et al., (2000). *Nature Cell Biology* **2**: 805-811.

Kang GX et al., (2003). *Journal of Biological Chemistry* **278**: 8279-8285.

We thank the British Heart Foundation for their support.

Authors have confirmed where relevant, that experiments on animals and man were conducted in accordance with national and/or local ethical requirements.

C43

Protease-activated receptor 2 mediates acute pain via PLC-dependent inhibition of Kv7 channels in nociceptive sensory neurons

J.E. Linley¹, K. Rose¹, B. Robertson¹, A. Akopian² and N. Gamper¹

¹Institute of Membrane and Systems Biology, University of Leeds, Leeds, UK and ²Department of Endodontics, University of Texas Health Science Center at San Antonio, San Antonio, TX, USA

Protease-activated receptor 2 (PAR2) is functionally expressed in sensory neurons and has been implicated in the pathophysiology of inflammation and pain. PAR2 signals through the $\text{G}_{\text{q/11}}$ class of G-proteins and phospholipase C (PLC) which hydrolyses membrane phosphatidylinositol 4,5-bisphosphate (PIP_2), releases InsP_3 and can trigger InsP_3 -mediated Ca^{2+} release from intracellular stores. One of the major contributors to the control of sensory neuron excitability is the M current, conducted by Kv7 channels, which are sensitive to changes in membrane PIP_2 and cytosolic Ca^{2+} . We therefore sought evidence for M current modulation by PAR2 in rat dorsal root ganglion (DRG) sensory neurons.

In whole cell perforated patch recordings from small DRG neurons in culture, bath application of 2f-LIGRLO-amide (10 μM), a peptide agonist of PAR2 (PAR2-AP) resulted in a dramatic and sustained reduction in M current of $80.5 \pm 11\%$ ($n = 23$, mean

$\pm \text{SEM}$, paired t-test, $p < 0.0001$) and a depolarisation of the resting membrane potential by $8.8 \pm 2 \text{mV}$. Confocal microscopy of DRG neurons transfected with an optical probe for PIP_2 (PLC δ -PH-GFP) revealed that PAR2-AP stimulated PIP_2 hydrolysis and InsP_3 production (7/12 neurons). Calcium imaging of DRG neurons revealed robust rises in $[\text{Ca}^{2+}]_i$ induced by PAR2-AP (43/131), by Ca^{2+} release from intracellular stores. The majority of PAR2-AP responsive neurons (36/43) also responded to the vanilloid receptor-1 agonist capsaicin, a biomarker for nociceptive neurons. Consistently, M current inhibition by PAR2-AP could be effectively blocked by edelfosine (PLC inhibitor, 10 μM , $13 \pm 4\%$ inhibition, $n = 6$). In addition, xestospongine C (InsP_3 receptor inhibitor, 1 μM , $18 \pm 9\%$ $n = 5$) and intracellular BAPTA (10 mM, $34 \pm 6\%$ $n = 14$) also markedly reduced inhibition of M current by PAR2-AP. Buffering changes in membrane PIP_2 with short-chain diC-8 PIP_2 (100 μM) in the patch pipette only modestly reduced M current inhibition ($64 \pm 3\%$ inhibition, $n = 4$), while buffering both Ca^{2+} and PIP_2 produced inhibition comparable with that of edelfosine ($24 \pm 6\%$ inhibition, $n = 14$). Inhibition of M current by PAR2 could be reproduced in a cell line overexpressing Kv7.2, Kv7.3 and PAR2. In behavioural studies, intraplantar injection of the selective M channel blocker, XE991 (2, 20 or 200 μM), into the rat hind paw produced prominent dose-dependent nociceptive behavior similar to that induced by injection of PAR2-AP (50 μM). However, co-injection of XE991 and PAR2-AP did not result in summation of pain.

These data indicate a novel pathway for protease induced inflammatory pain, namely PLC-mediated inhibition of M channels located in the peripheral nerve terminals. M-channel suppression may therefore contribute to the development of 'peripheral sensitization' in sensory neurons.

Supported by the Wellcome trust.

Authors have confirmed where relevant, that experiments on animals and man were conducted in accordance with national and/or local ethical requirements.

C44

Alzheimer's Disease: A result of the deterioration in K^+ channel homeostasis?

T.L. Kerrigan^{1,2}, C. Peers¹ and H.A. Pearson²

¹Division of Cardiovascular and Neuronal Remodelling, University of Leeds, Leeds, UK and ²Institute of Membrane and Systems Biology, University of Leeds, Leeds, UK

Accumulation of amyloid β ($\text{A}\beta$) peptides constitutes the neuropathological hallmark of Alzheimer's disease (AD). According to the amyloid hypothesis, the accumulation of $\text{A}\beta$ results in progressive loss of synaptic efficacy. K^+ channels regulate a number of processes: the resting potential, keeping action potentials short, timing interspike intervals and synaptic plasticity¹. A number of studies have shown that $\text{A}\beta$ alters properties of K^+ currents in neurons^{2,3,4}. We have previously reported a possible physiological role for

the soluble A β ₁₋₄₀ peptide in modulating 'A'-type K⁺ channels in cerebellar granule neurons^{3,4}. In this study we use organotypic hippocampal slices to mimic the *in vivo* modulation of K⁺ channels by soluble rat recombinant A β ₁₋₄₀ over 24 hours.

Whole-cell patch clamp measurements of K⁺ channel currents were carried out using organotypic hippocampal slices prepared from 8-10 day old rats using the Stoppini method⁵. The extracellular solution contained aCSF consisting of (mM): 126 NaCl, 3KCl, 1.25NaH₂PO₄, 2MgSO₄, 2CaCl₂·2H₂O, 10 glucose and 24 NaHCO₃. Intracellular solution contained (mM): 140KCl, 0.5CaCl₂, 5EGTA, 10HEPES and 2K-ATP. Rat recombinant A β ₁₋₄₀ was solubilised in DMSO before dilution in culture media to a concentration of 10nM and applied to slices for 24 hours. The reverse A β ₄₀₋₁ peptide was used as control. Statistical differences were assessed using repeated measures ANOVA with Tukey's post-hoc test or an unpaired Student's t-test.

Rat recombinant A β ₁₋₄₀ caused a significant 3.5 fold increase in the peak K⁺ channel current density/voltage (I-V) relationship in slices (n=6 controls, n=7 A β -treated cells). At a test potential of +50mV, current increased from 20.0±0.01 pA/pF in the control to 90.0±0.02pA/pF. Peak K⁺ channel current was further separated by their inactivation properties into fast inactivating 'A'-type(I_{KA}) and non-inactivating delayed rectifier (I_{KV}) components. In order to isolate the two components, cells were prepulsed to a potential of -140mV and measurements of the peak current was subtracted from the current at the end of the test step (peak-end). The I_{KA} component of the K⁺ current I-V was particularly sensitive to the effects of rat recombinant A β ₁₋₄₀, with a significant 5 fold increase in K⁺ channel current density when compared to the control. At a test potential of +50mV, current increased from 5.0±0.01 pA/pF in the control to 30.0±0.01 pA/pF in A β -treated cells. There was no significant difference in I_{KV}.

The data from this study corroborate our previous findings, supporting a physiological role for the A β ₁₋₄₀ peptide as a modulator of K⁺ channels, in particular the I_{KA} component. I_{KA} channels have been implicated in the onset of LTP in neurons, which is thought to underlie learning and memory¹. A disruption in this physiological modulation may therefore result in a disruption of synaptic plasticity, classic to AD.

Hoffman D.J. Magee JC, Colbert CM, Johnston D. K⁺ channel regulation of signal propagation in dendrites of hippocampal pyramidal neurons (1997). *Nature* Jun26;387(6636):869-75.

Yu HB, Li ZB, Zhang HX, Wang XL. Role of potassium channels in A β (1-40)-activated apoptotic pathway in cultured cortical neurons(2006). *J Neurosci Res.* Nov 15;84(7):1475-84.

Plant LD, Webster NJ, Boyle JP, Ramsden M, Freir DB, Peers C, Pearson HA. Amyloid beta peptide as a physiological modulator of neuronal 'A'-type K⁺ current. *Neurobiol Aging.* 2006 Nov;27(11):1673-83.

Kerrigan T.L., Atkinson L, Peers C., Pearson H.A. (2008) Modulation of 'A'-type K⁺ current by rodent and human forms of amyloid β protein. *NeuroReport* (In Press).

Stoppini L., Buchs P.A., Muller D. A simple method for organotypic cultures of nervous tissue. (1991) *J Neuroscience Methods.* 37;173-182.

Authors have confirmed where relevant, that experiments on animals and man were conducted in accordance with national and/or local ethical requirements.

Gating of a ClC chloride channel by voltage-dependent proton influx into the selectivity filter

L. Cid¹, M.I. Niemeyer¹, Y.R. Yusef¹, R. Briones¹, M. Catalán¹ and F.V. Sepúlveda^{1,2}

¹Centro de Estudios Científicos (CECS), Valdivia, Chile and ²Centro de Ingeniería de la Innovación, Valdivia, Chile

Membrane channels and transporters involved in moving ions into and out of cells are believed to function in fundamentally different ways. Ion channel function requires a continuous aqueous pore through the protein to allow ion migration by electrodiffusion plus some mechanism for opening and closing this pathway, the gate. Transporters, on the other hand, require at least two gates never simultaneously open that temporarily trap the ion within the pore. As might be expected from their functional differences, ion channels and transporters belong to different protein families. An exception to this rule occurs in the ClC transport protein family that, surprisingly, has both Cl⁻ ion channel and H⁺-coupled Cl⁻ transporter members. The strong conservation in structure within the ClC family suggests a degree of conservation in their molecular mechanisms (Dutzler, 2007). Available ClC structures reveal a selectivity filter providing a transmembrane pathway which is obstructed at its external opening by a highly conserved glutamate residue side-chain. A displacement of the selectivity filter glutamate clears the pathway to ion passage and is believed to be the process gating the pore in ClC channels. In the transporters, the equivalent residue serves to capture a proton to be translocated in exchange for Cl⁻ across the plasma membrane in a cycle of conformational changes not yet well defined. Here we show what appears like a partial reaction of such cycle accounting for the gating of ClC-2, a Cl⁻ channel member of the ClC family (Niemeyer et al., 2003; Yusef et al., 2006). Using a recombinant ClC-2 channel expressed in HEK-293 cells and analysed by patch-clamp, we demonstrate that ClC-2 channels, which are activated by hyperpolarisation, require protonation of the gate glutamate (E207 in ClC-2) in order to open. A Woodhull-type analysis suggests that E207 lies well within the electrical field of the membrane, making its neutralisation markedly voltage-dependent consistent with H⁺ entering the selectivity filter to effect activation, but not permeating across significantly. Intracellular Cl⁻, which also has an effect upon gating, acts in a permissive rôle, modulating the pH-dependence of channel opening in a voltage-independent manner. Our data are consistent with a model in which hyperpolarisation activates ClC-2 Cl⁻ channels by promoting H⁺ partial crossing of the selectivity filter to neutralise the gate glutamate residue thus allowing Cl⁻ permeation. This model upholds the view that ClC channels might have evolved from their exchanger counterparts conserving partial reactions of their transporter cycle.

Dutzler R (2007) *FEBS Lett* 581, 2839-2844.

Niemeyer MI et al. (2003) *J Physiol (London)* 553, 873-879.

Yusef YR et al. (2006) *J Physiol (London)* 572, 173-181.

Supported by Fondecyt 1070722 and 3080017. CECS is funded by the Millennium Science Initiative, Conicyt BFP and Gobierno Regional XIV.

Authors have confirmed where relevant, that experiments on animals and man were conducted in accordance with national and/or local ethical requirements.

C46

Developmental alternative splicing of the cardiac Na⁺ channel, Nav1.5

J.K. Diss^{1,2}, S.P. Barry¹, R. Onkal², J. Corness¹, J.H. Mattis², V.S. Budhram-Mahadeo¹, S.P. Fraser², M.B. Djamgoz² and D.S. Latchman¹

¹Medical Molecular Biology Unit, Institute of Child Health, London, UK and ²Neuroscience Solutions to Cancer, Imperial College, London, UK

From mid-gestation, action potentials (APs) are initiated by large transient inward Na⁺ currents (I_{Na}(T)), derived from voltage-gated Na⁺ channels (VGSCs), primarily Nav1.5 [1]. Nav1.5 can also produce a persistent Na⁺ current (I_{Na}(P)), in which the inactivation component is greatly slowed, which prolongs the cardiac AP and is a major pathway for intracellular Na⁺ entry [2]. We have found that Nav1.5 has two variants of exon 6 (a 5' genomic variant and a 3' variant), which encodes a region of the first transmembrane domain (D1) close to the S4 voltage-sensing segment [3]. This splicing has previously been described for other VGSCs. Splice forms typically only differ at one amino acid (position 7) [3]. The two Nav1.5 variants are unusual in that (i) they differ at 7 amino acids, and (ii) at position 7 of the 5'-variant, the characteristic neutral residue is replaced with a positively-charged lysine.

In the original report (of rat Nav1.2 splicing), transcripts with the 5' variant were abundant at birth but quickly replaced by 3'-variant containing transcripts within days. Thus 5'-variant channels were termed 'neonatal' and 3'-, 'adult' [4]. We initially found Nav1.5 splicing was similarly developmentally regulated in mouse hearts [2]. However, we did not investigate (a) whether 'neonatal' Nav1.5 (nNav1.5) was more abundant than 'adult' Nav1.5 (aNav1.5) in neonates, or (b) what changes occur in this splicing during embryonic and foetal development. Here we have used isoform-specific real-time RT-PCRs on mouse hearts from E9.5 to P19.5 to address this. Our data shows that aNav1.5 mRNA levels increase dramatically from E9.5 (~300-fold), peaking at P1.5. In contrast nNav1.5 levels remain relatively constant through to adulthood. nNav1.5 thus contributes proportionally more to cardiac Nav1.5 expression at early embryonic stages than in later development. However, since Nav1.5 at E9.5 is already of critical importance (as E9.5 Nav1.5 -/- mice already display severe cardiac abnormalities), nNav1.5, constituting ~50% of Nav1.5 mRNA at E9.5, is likely to have a major role in heart development.

Finally, to determine how Nav1.5 splicing changes relate to excitability changes in the developing heart, nNav1.5 and aNav1.5 channels were stably transfected into EBNA-293 cells and their electrophysiological properties compared. Importantly, differences between the two Nav1.5 isoforms were found that would be consistent with the previously reported loss of spontaneous AP firing and increase in I_{Na}(T) kinetics with development [5].

In conclusion, nNav1.5 is expressed at its highest level (proportionally) in the early embryonic heart and its electrophysiological properties are consistent with it making a significant contribution to heart excitability at this stage. The continued expression of this splice variant in adulthood might further suggest it is also important in the adult heart.

Kirby ML (2007). Cardiac Development. Oxford University Press.

Saint DA (2007). Br J Pharmacol 153, 1133-1142.

Fraser SP et al. (2005). Clin Cancer Res 11, 5381-5389.

Sarao R et al. (1991). Nucleic Acids Res 19, 5673-5679.

Itoh H et al. (2007). Syst Synth Biol 1, 11-23.

Authors have confirmed where relevant, that experiments on animals and man were conducted in accordance with national and/or local ethical requirements.

C47

Electrophysiological identification of epithelial sodium channels in canine articular chondrocytes

R. Lewis¹, A. Mobasheri² and R. Barrett-Jolley¹

¹Veterinary Pre-Clinical Science, University of Liverpool, Liverpool, UK and ²School of Veterinary Medicine and Science, University of Nottingham, Loughborough, UK

Amiloride-sensitive epithelial Na⁺ channels (ENaC) play a key role in Na⁺ transport and fluid homeostasis across the epithelia of the kidney, lung, and colon. ENaC is also known to be present in skin (Mauro *et al.*, 2002, Charles *et al.*, 2008) and articular cartilage (Trujillo *et al.*, 1999) although functional evidence for ENaC in articular cartilage is still lacking.

In the present study, inside-out patch clamp electrophysiology was used to identify ENaC-like unitary currents in isolated canine articular chondrocytes. Isolated chondrocytes were cultured for 7 to 9 days in Dulbeccos Modified Eagles Medium with 10% Foetal Calf Serum. Recording was carried out on first to third passage cells. Membrane potential (*V*_m) was calculated as *V*_m = -*H*_p-*V*_j

where *H*_p was the holding potential and *V*_j the calculated junction potential. Data is expressed as mean±standard error.

Single-channel activity reversed at a membrane potential of -1±5mV (*n* = 5) in the presence of 196mM internal and 155mM external Na⁺ solutions, indicative of a sodium current (calculated equilibrium potential, *E*_{Na} = -6mV). Mean slope conductance of the channel was calculated to be 9±0.4pS (*n* = 5). The ENaC-like channel activity was inhibited by the sodium-channel blocker amiloride at a concentration of 10µM. ENaC-like unitary currents were seen in approximately 60% of patches and had a mean open probability (*P*_o) of 0.3±0.06 (*n* = 3). After application of amiloride, channel *P*_o decreased by 97±2% (*n* = 3).

This study provides the first single channel electrophysiological evidence of functional ENaC expression in canine articular chondrocytes and supports previously published molecular evidence for the presence of ENaC in chondrocytes (Trujillo *et al.*, 1999).

Charles, R.P., Guitard, M., Leyvraz, C., Breiden, B., Haftek, M., Haftek-Terreau, Z., Stehle, J.C., Sandhoff, K., Hummler, E. (2008) Postnatal requirement of the epithelial sodium channel for maintenance of epidermal barrier function. J Biol Chem 283, 2622-2630

Mauro, T., Guitard, M., Behne, M., Oda, Y., Crumrine, D., Komuves, L., Rassner, U., Elias, P.M., Hummler, E. (2002) The ENaC channel is required for normal epidermal differentiation. *J Invest Dermatol* **118**, 589-594

Trujillo, E., Alvarez de la Rosa, D., Mobasheri, A., Gonzalez, T., Canessa, C.M., Martin-Vasallo, P. (1999) Sodium transport systems in human chondrocytes. II. Expression of ENaC, Na⁺/K⁺/2Cl⁻ cotransporter and Na⁺/H⁺ exchangers in healthy and arthritic chondrocytes. *Histol Histopathol* **14**, 1023-1031

This study was funded by the BBSRC.

Authors have confirmed where relevant, that experiments on animals and man were conducted in accordance with national and/or local ethical requirements.

C48

Development and validation of the QPatch medium-throughput patch clamp electrophysiology assay for brain sodium channel inhibitors

N. Garbati, R. Bonfante and C. Large

Neuropharmacology, GlaxoSmithKline, Verona, Italy

Sodium channel inhibition is an established mechanism that can confer anticonvulsant efficacy across a broad spectrum of seizure types [1-3]. However, a quantitative relationship between sodium channel inhibition and clinical anticonvulsant efficacy has yet to be determined. Traditional patch-clamp electrophysiology is the in vitro gold standard for measurement of compound activity on ion channels. However it has limited use for the evaluation of many drugs due to low throughput. The QPatch automated planar array patch-clamp system has been designed to increase throughput. The aim of this study was to develop and validate a robust electrophysiology assay using QPatch to define the interaction of drugs with recombinant human Nav1.2 sodium channels. In particular, to allow estimation of the affinity of drugs for the inactivated state of the channels (K_i). This value could then be used to explore the relationship between drug potency observed in vitro and brain concentration required for efficacy in vivo.

A first set of experiments was performed to assess assay fidelity and recording quality. A classic voltage step protocol was applied consisting of depolarising voltage steps (10 ms), increasing by 10 mV from -40mV to +40 mV from a holding potential of -90 mV. The I-V plot obtained suggests that the inward current reverses at around +50 to +60 mV, consistent with the reversal potential of sodium ions observed using a manual patch clamp assay. Secondly, the sensitivity of the QPatch assay to DMSO, used to dissolve test compounds, was assessed. The data obtained suggest that a maximum concentration of 0.3% can be reached without affecting recorded currents.

In a further set of experiments the viability of whole cell recordings over time was determined. For these experiments, test pulses to 0 mV were applied at a regular interval. Currents remained stable for at least 20 minutes.

Finally, a steady state inactivation protocol was applied to determine the affinity of compounds for the inactivated state (K_i) [4]. HEK-hNav1.2 cells were held at -120 mV and stepped to differ-

ent conditioning voltages (-120/-40 mV) for 9 s to induce steady state inactivation. At the end of each conditioning period the cell was stepped to +20 mV for 2 ms to elicit sodium current. For each recording, the peak current was plotted against the conditioning voltage and the data fitted to a Boltzmann equation from which the half-maximal inactivation voltage (V_h) could be determined. Application of drug caused a concentration-dependent leftward shift of the inactivation curve. By plotting the shift in V_h against drug concentration it was possible to estimate the K_i of the compound tested. The results show that the QPatch system provides a robust assay that can be used to evaluate the interaction of compounds with recombinant human Nav1.2 sodium channels.

Rogawski MA, Loscher W: The neurobiology of antiepileptic drugs. *Nat Rev Neurosci* 2004;5:553-564.

Catterall WA: Molecular properties of brain sodium channels: an important target for anticonvulsant drugs. *Adv Neurol* 1999;79:441-456.

White HS, Smith MD, Wilcox KS: Mechanisms of action of antiepileptic drugs. *Int Rev Neurobiol* 2007;81:85-110.

Kuo and Lu, Characterization of lamotrigine inhibition of Na⁺ channels in rat hippocampal neurones 1997, B.J.P. 121, 1231-1238

Authors have confirmed where relevant, that experiments on animals and man were conducted in accordance with national and/or local ethical requirements.

C49

Uncoupling protein 3 inversely correlates with resting metabolic rate in fit, young men

L.M. Edwards^{1,2}, N.S. Knight¹, C.J. Holloway^{1,2}, D. Woods¹, S. Tyler¹, A.J. Murray³, P.A. Robbins¹ and K. Clarke¹

¹Department of Physiology, Anatomy and Genetics, University of Oxford, Oxford, UK, ²Oxford Centre for Clinical Magnetic Resonance Research, John Radcliffe Hospital, Oxford, UK and ³Department of Physiology, Development and Neuroscience, University of Cambridge, Cambridge, UK

Uncoupling protein 3 (UCP3) is a mitochondrial protein found principally in skeletal and cardiac muscle, and thought to play a role in reducing reactive oxygen species (ROS) production via respiratory uncoupling. We therefore examined the relationships between UCP3, resting metabolism and oxidative modification of myocellular proteins in fit, young men.

METHODS: Twelve male subjects were recruited from the Oxford colleges' rowing crews. Resting metabolic rate (RMR) was estimated from respired gases during a ten-minute period of quiet sitting. Percutaneous needle biopsies were taken from the *m. vastus lateralis* of each subject under local anaesthetic (5ml of 2% Lidocaine), and snap-frozen in liquid nitrogen. UCP3, citrate synthase and ATP-synthase protein content were measured by western blotting. Protein carbonylation was measured using the DNPH-derivitization method of Levine *et al.*¹. All western blots were performed in duplicate.

RESULTS: We observed an inverse correlation between UCP3 and mass^{2/3}-adjusted RMR ($r = -0.63$, $P < 0.05$, $n = 12$, Fig. 1B). This relationship remained after UCP3 was normalised to either citrate synthase or ATP-synthase ($r = -0.66$ and $r = -0.69$, both

Siberian hamsters. Importantly these changes do not depend on the presence of sex hormones. We speculate that the increase in SR calcium content and thus calcium transient amplitude observed in SP animals may occur due to alterations in the phosphorylation status of phospholamban and that the increased SR mediated calcium uptake is a key step in protecting against cardiac arrhythmias during torpor.

This work was supported by The Biotechnology and Biological Sciences Research Council.

Authors have confirmed where relevant, that experiments on animals and man were conducted in accordance with national and/or local ethical requirements.

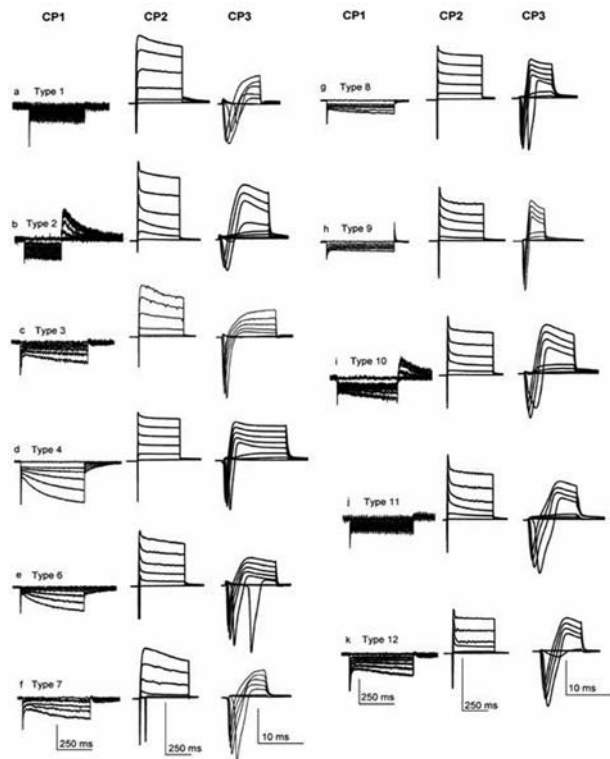
PC71

Electrophysiology of newborn rat primary sensory neurons in acute and organotypic dorsal root ganglia slices

P. Nicoleta, A. Bogdan and F. Maria Luisa

Animal Physiology and Biophysics, University of Bucharest, Faculty of Biology, Bucharest, Romania

Here we present the classification and algescic profile of newborn Wistar rat neurons from acute and organotypic dorsal root ganglia (DRG) slices, using previously defined electrophysiology protocols (1), with slight changes. Newborn rats (3–5 days) were anaesthetized on ice, decapitated and dissected in ice-cold bicarbonate Ringer. Both acute and cultured DRG slice protocols were described in our previous study (2). Whole cell recordings were performed during the same day for acute DRG slices and during the second day for cultured DRG slices. 114 acute DRG slice neurons and 111 organotypic DRG slice neurons were recorded and classified into 11 and 12 different types, respectively. Cell types 3, 5, and 7 were absent in acute DRG slices while cell types 2 and 9 were present only in acute DRG slices, and three other cell types (10, 11 and 12) were added to the classification (1). Concerning the algescic profile, we noticed increased capsaicin-activated currents (pA/pF) in culture vs. acute slices for type cells 1 (58.59 ± 4.06 vs. 30.36 ± 2.51) and 6 (29.21 ± 1.68 vs. 14.88 ± 2.69) and decreased for type cell 11 (38.51 ± 3.57 vs. 15.92 ± 0.56). Acid-activated transient currents (pA/pF) in organotypic slice neurons decreased for all type cells (type 4: 17.72 ± 2.74 vs. 7.54 ± 1.65 , type 6: 64.12 ± 4.43 vs. 22.01 ± 0.83 , type 8: 37.18 ± 6.41 vs. 2.48 ± 0.07 and type 11: 60.39 ± 6.51 vs. 4.01 ± 0.27), excepting type cell 1 where was observed an increase (3.8 ± 0.41 vs. 15.84 ± 1.22). ATP-evoked density currents remained unchanged in both acute and culture slices. In conclusion, data presented within the current report show differences in phenotype and excitability of cultured versus acute DRG slice neurons from newborn rat. Moreover, acute DRG slices offer an in vitro model closer to in vivo conditions, neurons in slices remaining in contact with other neurons and glial cells, like in ganglia of living animals.



Current signatures of neurons in newborn rat acute and organotypic DRG slices. Using very small (<22 μ m), small (24–32 μ m) and medium (32–45 μ m) DRG neurons from acute and organotypic slices, twelve different types were identified. CP1 and CP2 protocols were sufficient to distinguish types 1, 2, 4, 6 and 10. CP3 was used to distinguish between types 3 and 7, 9 and 11, 8 and 12. Vertical scale bars: for CP1: 250 pA (a), 150 pA (b), 150 pA (c), 500 pA (d), 100 pA (f), 200 pA (g), 150 pA (h), 250 pA (i), 100 pA (j), 100 pA (k), 300 pA (l); for CP2: 4000 pA (a), 6000 pA (b), 2500 pA (c), 4500 pA (d), 3000 pA (f), 4000 pA (g), 4000 pA (h), 5000 pA (i), 6000 pA (j), 7000 pA (k), 5000 pA (l); for CP3: 8000 pA (a), 6000 pA (b), 4000 pA (c), 4000 pA (d), 5000 pA (f), 7500 pA (g), 5000 pA (h), 5000 pA (i), 3000 pA (j), 4000 pA (k), 6000 pA (l). Petruska JC, Napaporn J, Johnson RD, Gu JG, Cooper BY. J. Neurophysiol. 84:2365–2379, 2000

Neacsu N, Flonta ML. Romanian J. Biophys. 16, 2: 77–91, 2006

To Prof. Dr. ML Flonta my PhD supervisor and Conf. Dr. B Amuzescu

Authors have confirmed where relevant, that experiments on animals and man were conducted in accordance with national and/or local ethical requirements.

PC72

Involvement of transient receptor potential melastatin 7-like channels in survival of human gastric cancer cell

B. Kim¹, E. Park¹, J. Lee¹, J. Jeon¹, S. Kim² and I. So¹

¹Center for Bio-Artificial Muscle and Department of Physiology, Seoul National University College of Medicine, Seoul, South Korea and ²Center for Bio-Artificial Muscle and Department of Biomedical Engineering, Hanyang University, Seoul, South Korea

Ion channels are involved in normal physiologic processes and in the pathology of various diseases. In this study, we investi-

gated the presence and potential function of transient receptor potential melastatin 7 (TRPM7) like channels in the survival of AGS cells, human gastric adenocarcinoma cells, using a combination of patch-clamp recording, RT-PCR, western blotting, small interfering RNA (siRNA), and MTT (thiazolyl blue tetrazolium bromide) assay. AGS cells have been found to express endogenously TRPM7 like current. This current can be inhibited by La³⁺, 2-aminoethoxydiphenyl borate (2-APB), or intracellular Mg²⁺, consistent with the TRPM7 current being activated. Reverse transcription-PCR and western blotting detected the expression of TRPM7 mRNA and protein in these cells. Transfection of AGS cells with TRPM7 siRNA significantly reduced the expression of TRPM7 protein and TRPM7 like current. Furthermore, we found that TRPM7 like current is critical for the survival of AGS cells. Blockade of TRPM7 like channels by La³⁺ and 2-APB or suppression of TRPM7 expression by siRNA inhibited the survival of these cells. In summary, AGS cell lines express the nonselective cation channel TRPM7 whose presence is essential for cell survival.

This work was supported by the Creative Research Initiative Center for Bio-Artificial Muscle of the Ministry of Science & Technology (MOST) / the Korea Science and Engineering Foundation (KOSEF).

Authors have confirmed where relevant, that experiments on animals and man were conducted in accordance with national and/or local ethical requirements.

PC73

Analysis of P2X4 and P2X7 receptor complexes for heterologously over expressed and endogenously expressed receptors

M. Masin, A. Paramasivam, M. Boumechache, N. Barrera, M. Edwardson and R. Murrell-Lagnado

Pharmacology, University of Cambridge, Cambridge, UK

Mammalian P2X receptors are formed by seven subunits (P2X1 to P2X7) that can arrange as homo- or heterotrimers. P2X7 receptors play an important role in the physiology of the immune system, with key roles in mechanisms such as cytokine release, apoptosis and microbial killing. This receptor is frequently co-expressed in immune cells with another member of the P2X family, the P2X4 receptor. The role of P2X4 receptor in immune cells is not as well understood although its up-regulation in spinal cord microglia, as a result of peripheral nerve injury, contributes to neuropathic pain.

We recently provided biochemical and electrophysiological evidence of a structural and functional association between P2X4 and P2X7 receptors (Gou et al. 2007). What is not yet known is whether or not individual subunits interact to form heterotrimeric receptors, or if mature homomeric receptors associate in higher order complexes. Analysis of P2X4 and P2X7 receptors heterologously expressed in HEK293 cells by blue native (BN)-PAGE, show that both form stable trimeric complexes and that P2X4, but not P2X7, also appears to form stable hexamers and nonamers as described previously (Aschrafi

et al. 2004). Analysis of P2X4 receptors from bone marrow derived macrophages (BMDMs) showed no band corresponding in size to either trimers or hexamers but instead a predominant band of intermediate size, ~100 kDa larger than predicted for a P2X4 trimer. Following partial dissociation a band corresponding in size to the trimer was seen suggesting that the endogenous P2X4 receptors are forming a complex with other protein(s). Cross-linking of surface receptors in microglia followed by SDS-PAGE and western blot with an anti-P2X4 antibody similarly showed a predominant band that was considerably larger than a trimer. A band of the same size was also recognized by the anti-P2X7 antibody, suggesting that the endogenous complexes contain both P2X4 and P2X7. Further analysis of P2X receptor complexes purified from HEK293 cells are being carried out using atomic force microscopy (AFM).

Gou et al. (2007) *Mol Pharmacol* 72(6), 1447-56

Aschrafi et al. (2004) *J Mol Biol* 342(1), 333-43

Authors have confirmed where relevant, that experiments on animals and man were conducted in accordance with national and/or local ethical requirements.

PC74

N-Glycosylation-dependent control of K2P3.1 membrane expression

I. O'Kelly and D. Johnson

Faculty of Life Sciences, University of Manchester, Manchester, UK

K2P3.1 mediates background potassium currents, and therefore reduced membrane expression of these channels will impair the function of electrically excitable cells. Understanding the mechanisms by which these channels are trafficked to the cell membrane is of vital importance to the understanding of K2P3.1-related channelopathies. Glycosylation is a critical modulator of sodium and potassium channel gating and trafficking. As K2P3.1 is a predicted glycoprotein with one external N-glycosylation site, we therefore investigated whether N-glycosylation has effects on K2P3.1 membrane expression. The N-glycosylation site was deleted using site-specific mutagenesis. Gel shift assays were performed with wild-type K2P3.1 and the N-glycosylation deficient mutant (K2P3.1N53Q) purified from the membrane fraction of COS-7 cells transiently expressing the channels. The molecular weight of K2P3.1N53Q was lighter compared to wild-type K2P3.1 demonstrating that the N-glycosylation site was occupied and that N-glycosylation accounted for approximately 5-10% of the total mass of K2P3.1. When internal GFP- and external HA-tagged-K2P3.1 and -K2P3.1N53Q were transiently expressed in COS-7 cells approximately equal transfection efficiencies was achieved for both constructs (48% and 43%, respectively). However, wild-type K2P3.1 had enhanced membrane expression compared to K2P3.1N53Q, 89% vs. 61% of transfected cells, respectively, as determined by immunofluorescence using an anti-HA antibody. Chronic inhibition of N-glycosylation using tunicamycin also prevented customary membrane expression of K2P3.1 consistent with that seen for K2P3.1N53Q. These data demonstrate that N-

glycosylation is an integral component of K2P3.1 and has an important function in determining K2P3.1 channel stability and/or trafficking to the membrane with important physiological implications.

This work was supported by a Wellcome Trust Value In People Award.

Authors have confirmed where relevant, that experiments on animals and man were conducted in accordance with national and/or local ethical requirements.

PC75

Caveolin-1 modulates rat arterial ATP-sensitive potassium (K_{ATP}) channel activity

L. Davies¹, G.I. Purves¹, R. Barrett-Jolley² and C. Dart¹

¹School of Biological Sciences, University of Liverpool, Liverpool, UK and ²Department of Veterinary Preclinical Science, University of Liverpool, Liverpool, UK

ATP-sensitive K^+ channels (K_{ATP} channels) of arterial smooth muscle are critical regulators of arterial tone, and so blood flow, in response to vasoactive transmitters [1]. Recent biochemical evidence suggests that these channels localise to cholesterol and sphingolipid-enriched invaginations of the smooth muscle surface membrane termed caveolae [2]. These specialised lipid microdomains are thought to assist in the spatial organisation of signal transduction pathways by aggregating interacting proteins into functional signalling compartments [3]. Here we investigate the potential role of the caveolae-associated scaffold protein caveolin in regulating K_{ATP} channel activity. Immunogold electron microscopy of rat aortic smooth muscle plasma membrane sheets confirmed the presence of Kir6.1, the pore-forming inwardly rectifying subunit of the vascular K_{ATP} channel, in morphologically identifiable caveolin-rich regions of the membrane. Antibodies directed against vascular K_{ATP} channel subunits (Kir6.1 and sulphonylurea receptor (SUR2B)) co-immunoprecipitated caveolin-1 from rat aortic homogenates, suggesting that caveolin-1 interacts with the channel protein. To investigate whether this interaction has any functional effect on K_{ATP} channel activity pinacidil-evoked recombinant whole-cell K_{ATP} currents were recorded in HEK293 cells. Whole-cell K_{ATP} currents recorded at -60 mV in HEK293 cells stably expressing caveolin-1 were significantly smaller than currents recorded in wild-type HEK293 where caveolin is absent (69.6 ± 8.3 pA/pF, $n=8$; 179.7 ± 35.9 pA/pF, $n=6$, respectively; mean \pm SEM; $p<0.05$, Student's t test). In cell-attached patch clamp recordings, the presence of caveolin-1 had no significant effect upon pinacidil-evoked single K_{ATP} channel chord conductance (39.4 ± 2.5 pS, $n=5$; 30.6 ± 4.2 pS, $n=5$, respectively; membrane potential -60 mV; $p>0.05$, Student's t test). However, analysis of open and closed time distributions revealed that in the presence of caveolin-1 the channel spends significantly more time in longer-lived closed states ($p<0.05$, Student's t test).

Together these findings suggest that interaction with caveolin-1 has an inhibitory effect on vascular K_{ATP} channel activity that may be important in the physiological control of channel function.

Quayle JM et al. (1997). *Physiol Rev* 77, 1165-1232.

Sampson LJ et al. (2004). *Circ Res* 95, 1012-1018.

Razani B et al. (2002). *Pharmacol Rev* 54, 431-467.

This work is supported by the BBSRC and the BHF.

Authors have confirmed where relevant, that experiments on animals and man were conducted in accordance with national and/or local ethical requirements.

PC76

Stoichiometry and function of acid-sensitive K_{2p} channels

E.J. Lowry and I. O'Kelly

University of Manchester, Manchester, UK

Acid-sensitive background two-pore potassium channels (K_{2p}) are important contributors to the maintenance of cellular resting membrane potential and cellular excitability. Membrane expression of acid-sensitive K_{2p} channels, $K_{2p3.1}$, $K_{2p9.1}$ and $K_{2p15.1}$ is mediated by phosphorylation dependent trafficking by cytosolic protein 14-3-3. Loss of 14-3-3 interaction results in impaired membrane expression that could result in disrupted cellular excitability. We used two-electrode voltage-clamp to measure the functional activity of the acid-sensitive K_{2p} channels. *Xenopus laevis* oocytes expressing $K_{2p3.1}$ or $K_{2p9.1}$ exhibited a pH-dependent current, typical of acid-sensitive K_{2p} channels, however no current was seen in oocytes expressing $K_{2p15.1}$. $K_{2p3.1}\Delta V_{411}$ and $K_{2p9.1}\Delta I_{396}$ mutants, which have disrupted 14-3-3 binding sites, displayed significantly reduced current. $K_{2p3.1}\Delta V_{411}$ tagged with green fluorescent protein (eGFP) was transfected into COS-7 cells and imaged using immunofluorescence microscopy. Co-staining transfected cells with markers for the ERGIC and golgi using ERGIC-53 and GM-130 respectively did not show co-localisation in the majority of cells. $K_{2p3.1}\Delta V_{411}$ was shown to be localised to the endoplasmic reticulum (ER) by co-staining for the ER marker protein disulphide isomerase. The mutant $K_{2p3.1}\Delta V_{411}$ was able to overcome ER retention by co-expressing with wildtype $K_{2p3.1}$, $K_{2p9.1}$ or $K_{2p15.1}$. This data suggests that when 14-3-3 cannot bind $K_{2p3.1}$ is retained in the ER, but can be rescued by co-expression with wildtype channel and hence suggests the stoichiometry of interaction of 14-3-3. Furthermore this also demonstrates heterodimerisation of $K_{2p3.1}$ and $K_{2p15.1}$. Physiological significance of these results are far reaching as $K_{2p3.1}$ and $K_{2p15.1}$ demonstrate co-expression in an array of tissues such as the pancreas, placenta, kidney and lung.

Authors have confirmed where relevant, that experiments on animals and man were conducted in accordance with national and/or local ethical requirements.

PC77

The effects of ethanol on rat recombinant NR1/NR2A and NR1/NR2B N-methyl-D-aspartate receptors expressed in *Xenopus laevis* oocytes

H.J. Spencer-Otton, A. Janssen, C.A. Puddifoot, P.E. Chen and D.J. Wyllie

Centre for Neuroscience Research, University of Edinburgh, Edinburgh, UK

It is well-established that N-methyl-D-aspartate receptors (NMDARs) are inhibited by ethanol. However many studies that investigate the effects of ethanol on this receptor use concentrations of ethanol that would likely prove to be lethal in many individuals (100 mM and greater). To put this in context, in the UK the legal blood alcohol limit for driving a motor vehicle is 80 mg/100 ml which is equivalent to approximately 17 mM ethanol. Since NR2B-containing NMDARs are expressed earlier in neural development than NR2A-containing NMDARs, differential sensitivity of these NMDAR subtypes to ethanol may have implications for fetal exposure to ethanol during pregnancy. In our study we have examined the effects of ethanol (10, 20, 40 and 80 mM) on NR2A- and NR2B-containing NMDARs expressed in *Xenopus laevis* oocytes using two-electrode voltage-clamp recording techniques.

Control recordings from uninjected oocytes showed that the range of ethanol concentrations used did not affect the holding current required to voltage-clamp oocytes at -40, -60 or -80 mV in either a Ca^{2+} -containing or Ba^{2+} -containing external recording solution ($n = 11, 13$ respectively). For NR1/NR2A NMDARs ethanol (40 mM) inhibited glutamate-evoked (100 μM) currents in a voltage-independent manner (mean inhibition at -80 mV = $18.2 \pm 1.1\%$, $n = 21$). Similar levels of inhibition were observed for NR1/NR2B NMDARs (mean inhibition at -80 mV = $17.7 \pm 1.9\%$, $n = 17$). Concentration-response curves to determine the potency of glutamate and the co-agonist, glycine (in the presence of 40 mM ethanol) at NR1/NR2A and NR1/NR2B NMDARs demonstrated that the EC_{50} values obtained were not different from values previously reported (Erreger *et al.* 2007; Chen *et al.* 2008) for these receptor subtypes (NR2A: glut = $2.9 \pm 0.1 \mu\text{M}$, gly = $0.84 \pm 0.05 \mu\text{M}$; NR2B: glut = $1.4 \pm 0.1 \mu\text{M}$, gly = $0.74 \pm 0.07 \mu\text{M}$; $n = 9, 16, 8, 8$, respectively). Neither voltage-dependent Mg^{2+} block nor memantine block of glutamate-evoked currents mediated by either receptor subtype was affected by ethanol (40 mM). Thus under our recording conditions we find no evidence for a differential effect of the inhibitory action of ethanol at these two NMDAR subtypes.

Reduced ethanol inhibition of NR1/NR2A NMDAR-mediated responses was observed when the carboxy-terminus of the NR2A subunit was either deleted with the sequence ending at residue Phe822 (mean inhibition at -80 mV: $11.6 \pm 0.8\%$, $n = 8$) or truncated with the sequence ending at residue Iso1098 (mean inhibition at -80 mV: $10.7 \pm 1.8\%$, $n = 8$). The reduced inhibition seen with these NR2A carboxy-terminus deleted and truncated constructs suggests that this region of the NR2A subunit may contain sites of interaction with ethanol.

Chen *et al.* (2008). *J Physiol* **586**, 227-245.

Erreger *et al.* (2007). *Mol Pharmacol* **72**, 907-920.

This work was supported by funds from the Honours Programmes in Pharmacology and Neuroscience at the University of Edinburgh.

Authors have confirmed where relevant, that experiments on animals and man were conducted in accordance with national and/or local ethical requirements.

PC78

Effects of TARPs on basic properties of calcium-permeable AMPA receptors

D. Soto, I.D. Coombs, M. Zonouzi, M. Farrant and S.G. Cull-Candy

The Research Department of Neuroscience, Physiology and Pharmacology, Division of Biosciences, University College London, London, UK

Glutamate is the principal neurotransmitter in the brain, mediating fast synaptic transmission through AMPA-type glutamate receptors (AMPA receptors). Four receptor subunits (GluR1-4) form AMPA channels, the properties of which differ depending on RNA editing, alternative splicing and subunit composition. Furthermore, AMPA receptor properties critically depend on the presence of AMPAR auxiliary proteins. These transmembrane AMPAR regulatory proteins (TARPs) control both AMPA receptor trafficking and gating (Nicoll *et al.*, 2006). We have recently shown that the prototypical TARP, stargazin (γ -2), increases single channel conductance of Ca^{2+} -permeable AMPARs (CP-AMPA receptors). Moreover, it attenuates block of CP-AMPA receptors by intracellular polyamines, resulting in a decreased inward rectification of the current-voltage (I-V) relationship (Soto *et al.*, 2007). Five TARPs have been identified (γ -2, -3, -4, -7 and -8). Here we describe that all TARP family members modify basic properties of CP-AMPA channels.

We used a piezoelectric controller to apply brief pulses (100ms) of glutamate (10mM) to outside-out patches from tsA-201 cells transiently transfected with GluR4 subunits and TARPs. Non-stationary noise analysis of GluR4 responses yielded a weighted-mean single-channel conductance of $17.8 \pm 1.5\text{pS}$ ($n=4$). This conductance was increased by approximately 50% when GluR4 was coexpressed with the various different TARPs (e.g. GluR4 + γ -8, $34.1 \pm 4.5\text{pS}$; $n=4$); similar changes were obtained for all TARPs tested ($P < 0.01$ for all vs control). Furthermore, all TARPs slowed the desensitization kinetics of AMPARs, with the exception of the most recently described TARP family member γ -7 (GluR4 $\tau = 3.9 \pm 0.4\text{ms}$, $n = 4$; GluR4 + γ -7, $\tau = 3.6 \pm 0.5\text{ms}$ $n=3$); γ -4 and -8 gave the largest change in desensitization kinetics ($\tau = 9.31 \pm 1.9\text{ms}$ $n=5$ and $9.69 \pm 3.56\text{ms}$ $n=4$, respectively). Furthermore, all TARPs decreased spermine sensitivity of GluR4, altering the I-V relationship, although the extent of the decrease varied between the TARPs, with γ -3 causing the greatest reduction in rectification (RI (+60/-80): 0.02 ± 0.01 , $n=5$ for control vs. 0.34 ± 0.02 , $n=4$ for γ -3 ($P < 0.001$)).

Our experiments demonstrate that, in common with stargazin, other TARPs modify the biophysical properties of CP-AMPA receptors, and that the extent of the change varies between TARPs. As the type of TARPs expressed varies between brain areas (Tomita

et al., 2003), our results suggest that CP-AMPA receptors may be differentially modulated in different cell types.

Nicoll RA, Tomita S & Brecht DS (2006). *Science* 311, 1253-1256.

Soto D, Coombs ID, Kelly L, Farrant M & Cull-Candy SG (2007). *Nat Neurosci* 10, 1260-1267.

Tomita S, Chen L, Kawasaki Y, Petralia RS, Wenthold RJ, Nicoll RA, Brecht DS (2003). *J Cell Biol* 161, 805-816.

This work was supported by the Wellcome Trust, MRC and the Royal Society (SGC-C).

Authors have confirmed where relevant, that experiments on animals and man were conducted in accordance with national and/or local ethical requirements.

PC79

Trafficking of potassium voltage-gated ion channels in the neuroblastoma cell line SH-SY5Y via hypoxic modulation and its relationship to Alzheimer's disease

D.A. Beccano-Kelly¹, C.J. Milligan¹, C. Peers² and H.A. Pearson¹

¹Faculty of Biological Sciences, University of Leeds, Leeds, UK and

²Institute of Cardiovascular Medicine, University of Leeds, Leeds, UK

In Alzheimer's disease (AD) the most prevalent dementia in the western world, levels of the soluble peptide, amyloid beta (A β) are increased in the cerebral spinal fluid^{1,2}.

Elevation of this peptide has also been found in sufferers of strokes and other vascular disorders^{3,4}.

There is a strong positive correlate between the incidence of AD and those people who have had a prior ischemic episode⁵.

To clearly define the link between these two afflictions, the human neuroblastoma cell line SH-SY5Y, was used as a neuronal model, and were either hypoxically incubated, or transfected with known AD related mutations. High-throughput planar patch clamp technique has been employed to analyse K⁺ channel current. Biotinylation followed by western blot, probing for Kv3.1b, was also used to detect any changes in protein localisation.

Results show that cells containing Presenilin-1 (PS-1) mutations (e.g. D385N) and hypoxically treated cells both have elevated K⁺ channel current density; 79 ± 16 pA/pF (n=38) and 31 ± 12 pA/pF (n=5) at 50mV respectively, versus the control group, 16.5 ± 1.8 pA/pF (n=3). This functional elevation in current can be explained by an increase in membrane localisation of voltage gated potassium channels, as indicated by the biotinylation assay. This effect is ablated when one of the enzymes key to generating A β (γ -secretase) is inhibited. This data indicates a mechanism for the initiation of sporadic AD as a result of ischemic episodes, and also illustrates a role for A β in the homeostatic control of ions in neurons.

Borchelt DR, et al. (1996). *Neuron* 17, 1005.

Nakamura T. et al. (1994). *Ann Neurol* 36, 903-911.

Mattson MP. (1997). *Neuroscience & Biobehavioral Reviews* 21, 193.

Cole SL & Vassar R. *Neurobiology of Aging* In Press.

Kokmen EW et al. (2006). *Neurology* 46 (1): 154.

Thanks to the MRC for funding the project.

Authors have confirmed where relevant, that experiments on animals and man were conducted in accordance with national and/or local ethical requirements.

PC80

Failure of NMDAR activation during quantal release at cerebellar mossy fibre-granule cell synapses in adult mice

R. Ali¹, M. Renzi¹, M. Fukaya², M. Watanabe², M. Farrant¹ and S.G. Cull-Candy¹

¹The Research Department of Neuroscience, Physiology and Pharmacology, Division of Biosciences, University College London, London, UK and ²Department of Anatomy, Hokkaido University Graduate School of Medicine, Sapporo, Japan

At many excitatory synapses in the CNS, glutamate activates both AMPA- and NMDARs. Although it is commonly assumed that these receptors are co-localized in the postsynaptic membrane, the situation at adult synapses is unclear. Our studies of cerebellar granule cells (GCs) show that in immature animals NMDARs are activated during both spontaneous mEPSCs and following mossy fibre (MF) stimulation. By contrast, in mature mice, MF activity leads to activation of NMDARs (predominantly NR2C-containing; Cathala et al. 2000) but mEPSCs lack an NMDAR-mediated component (Cathala et al. 2003). Here we re-examined mEPSCs and evoked EPSCs in GCs from young and mature mice, and undertook EM immunogold localization of NMDARs, to investigate the presence and localization of NMDARs in GCs of adult mice.

Patch-clamp recordings were made from GCs in cerebellar slices from immature (P7-9) or mature (P34-55) mice, at 35°C. While mEPSCs were readily detected in Mg²⁺ free conditions at -70mV at both ages, these events were abolished in mature GCs by CNQX (non-NMDAR blocker), suggesting that at this age GCs lack synaptic NMDARs. To determine if NMDARs are present in the synaptic membrane, but have their activity suppressed, we examined mEPSCs under conditions that increase the likelihood of activating and detecting NMDAR currents. We examined cells in extracellular Mg²⁺ (at +30mV) to enhance NMDAR activation, with increased glycine to maximize activation of the NMDAR glycine site, in conditions that suppress tonic H⁺ inhibition of NMDARs and in conditions that suppress mGluR inhibition of NMDARs. No NMDAR-mediated component was seen in any of these conditions. This was also the case when Sr²⁺ was used to desynchronize release and enable examination of MF-evoked quantal events, suggesting that this discrepancy does not reflect a difference between spontaneous and evoked release.

Mature GCs are thought to express mRNA for both NR2C and NR2A. Consistent with this, we found both high- (50pS) and low conductance (19 and 38pS) NMDAR channels in outside-out patches from these cells. Immunogold labeling confirmed the presence of multiple NMDAR subunit types in the extrasynaptic membrane, and revealed a high particle density at intraglomerular non-synaptic attachment plaques (between adjacent dendrites). NR1, NR2A and NR2C labeling was also detected within postsynaptic densities (PSD), but at much lower

level. Overall our data suggest that either the sparse labeling of PSD does not reflect the presence of functional receptors, or the level of synaptic NMDAR expression is below that which can be resolved during our recordings. Alternatively, NMDARs are present but not activated during the brief glutamate transient arising from the release of single quanta. Future modeling studies will address this question.

Cathala L, Misra C & Cull-Candy SG. (2000) Developmental profile of the changing properties of NMDA receptors at cerebellar mossy fiber-granule cell synapses. *Journal of Neuroscience*, 20(16):5899-905.

Cathala L, Brickley S, Cull-Candy SG & Farrant M. (2003) Maturation of EPSCs and intrinsic membrane properties enhances precision at a cerebellar synapse. *Journal of Neuroscience*, 23(14):6074-85.

Supported by the Wellcome Trust, MRC and Royal Society.

Authors have confirmed where relevant, that experiments on animals and man were conducted in accordance with national and/or local ethical requirements.

PC81

Sheep RyR2 channel activity is regulated by an endogenous kinase other than PKA or CaMKII; an effect not mediated by S2809

S. Carter and R. Sitsapesan

Physiology & Pharmacology, University of Bristol, Bristol, UK

Previously we have demonstrated that PKA-dependent phosphorylation at S2809 is associated with a significant increase in RyR2 channel open probability (Po), and characteristic changes in gating¹. To further investigate RyR2 phosphorylation, sarcoplasmic reticulum vesicles were isolated² from sheep hearts obtained from an abattoir and were either incorporated into artificial membranes for single-channel studies or used for Western blot¹. In the presence of 50µM cytosolic free Ca²⁺, 5 min incubation with 5mM Mg²⁺ and 1mM ATP, followed by wash out to control conditions, significantly increased channel Po (from 0.071±0.023 to 0.334±0.076 (SEM; n=17, p<0.01, Student's t-test)). The increase in Po however, was smaller than that observed when exogenous PKA was included in the incubation medium (from 0.126±0.035 to 0.574±0.106 (SEM; n=10). Closer examination of the individual Mg²⁺ATP treated channels suggested the presence of two different sub-populations of RyR2. In 10 of 17 channels, Mg²⁺ATP treatment resulted in an increase in channel Po and a change in channel gating similar to that observed after PKA-dependent phosphorylation (Po rose from 0.033±0.011 to 0.534±0.079 (SEM; n=10). In the remaining channels, Mg²⁺ATP had no sustained effect (n=7). ATP alone, in the absence of Mg²⁺, produced a fully reversible increase in Po in all channels treated (n=12). It is possible that the heterogeneous response of the channels to Mg²⁺ATP is due to the close association of an endogenous kinase with some of the RyR2 channels reconstituted into bilayers. Use of the PKA inhibitor, PKI (10 µM), did not prevent the Mg²⁺ATP dependent increase in channel Po although it does prevent the effects of exogenously added PKA. Similarly the Ca²⁺/calmodulin-dependent protein kinase (CaMKII) inhibitor, autocamtide-2 related inhibitory peptide II (AIP II) (50 nM), did not prevent

the increase in Po at concentrations expected to inhibit CaMKII. Increasing the concentration of AIP II to a level reported to inhibit the action of PKC (1 µM) however, prevented the irreversible Mg²⁺ATP-induced changes. Further, use of the PKC specific inhibitor, chelerythrine chloride, also prevented the Mg²⁺ATP related change in channel activity. In the presence of 1µM chelerythrine chloride, Po was 0.120±0.039 before and 0.044±0.021 after treatment with Mg²⁺ATP (SEM; n=7). Chelerythrine chloride alone had no effect on channel Po. Although chelerythrine chloride inhibited the Mg²⁺ATP-dependent increase in channel Po, it did not prevent phosphorylation of RyR2 at S2809. Western blot analysis demonstrated that under lipid bilayer comparable conditions, only PKI prevented Mg²⁺ATP phosphorylation of S2809. We conclude that RyR2 channels may be associated with and phosphorylated by an endogenous kinase, possibly PKC, which does not appear to phosphorylate S2809.

Carter, S. et al. (2006). *Circ Res*, 98:1506-1513.

Kermode, H. et al. (1998). *FEBS Lett*, 431, 59-62.

Supported by the BHF.

Authors have confirmed where relevant, that experiments on animals and man were conducted in accordance with national and/or local ethical requirements.

PC82

Post-natal developmental changes in ion channel and Ca²⁺ handling protein expression in the ventricle

E.S. H Abd Allah, J.O. Tellez, T.A. Nelson, H. Dobrzynski and M.R. Boyett

University of Manchester, Manchester, UK

Transmural gradients in action potential duration (APD) and Ca²⁺ handling proteins are important for both the normal functioning of the ventricle and arrhythmogenesis. In the rabbit, the transmural gradient in APD is minimal in the neonate. During post-natal development, APD increases both in the epicardium and the endocardium, but the prolongation is more substantial in the endocardium leading to a significant transmural gradient. We have investigated changes in ion channel expression in the subepicardial and subendocardial layers of the left ventricular free wall in neonatal (2-7 days of age; n=11) and adult male (~6 months of age; n=11) New Zealand White rabbits using quantitative PCR (qPCR), *in situ* hybridisation (ISH) and immunohistochemistry. The rabbits were killed humanely in accordance with the regulations of the United Kingdom Animals (Scientific Procedures) Act 1986. qPCR revealed that in the neonate, Nav1.5 (responsible for I_{Na}), ERG (responsible for I_{Kr}) and minK (responsible for I_{Ks}) mRNAs were more abundant in the endocardium than the epicardium, whereas the reverse was true for KCHIP2 (in part responsible for I_{to}) mRNA. Moreover, in the adult, Cav1.2 (responsible for I_{CaL}), SERCA2a, RyR2, ERG, KvLQT1 (responsible for I_{Ks}) and KCHIP2 mRNAs were more abundant in the epicardium than the endocardium. Consistent with this, ISH

showed that KCHIP2 mRNA was more abundant in the epicardium than the endocardium both in the neonate and adult. However, in the neonate, whereas Nav1.5 mRNA was more abundant in the endocardium than the epicardium, it was uniformly distributed across the ventricle in adult. Cav1.2 mRNA was uniformly distributed across the neonatal ventricle, while in the adult ventricle, Cav1.2 mRNA was significantly more abundant in the epicardium than the endocardium. Immunohistochemistry confirmed that NCX1, SERCA2a and RyR2 proteins were more abundant in the epicardium than the endocardium in the adult, but not in the neonate. To conclude, there are complex developmental changes in ion channel and Ca^{2+} handling protein expression across the ventricle that may have implications for the treatment of arrhythmias.

Authors have confirmed where relevant, that experiments on animals and man were conducted in accordance with national and/or local ethical requirements.

PC83

Regulation of plasma membrane expression of P2X4 receptors in immune cells

M. Boumechache, A. Paramasivam, M. Masin and R. Murrell-Lagnado

Pharmacology, University of Cambridge, Cambridge, UK

P2X4 receptors are one of the predominant subtypes of purinergic receptors expressed in macrophages and microglia and their up-regulation has been shown to contribute to neuropathic pain. P2X4 receptors are prominently localized to lysosomes and resist degradation by virtue of N-linked glycans decorating the intra-luminal loop of the receptor. In order to understand how the expression of these receptors at the plasma membrane is regulated, we compared the proportion of receptors expressed at the cell surface in cultured microglia and macrophages following exposure to modulators of microglial/macrophage activation. Surface expression was analysed by biotinylation of exposed proteins and by cross-linking proteins with membrane impermeant cross-linkers, followed by SDS-PAGE and western blotting. The modulators included lipopolysaccharide (LPS), ATP and phorbol esters. A 24h incubation with LPS (500ng/ml) resulted in an up-regulation of P2X4 surface expression in cultured microglia without an evident increase in total expression of the receptor, indicating redistribution from intracellular compartments to the plasma membrane. In contrast, similar exposure of cultured astrocytes to LPS had no effect on the surface expression of P2X4 receptors. Exposure of microglia to LPS was sufficient to inhibit proliferation and we have compared the involvement of the P2X7 receptor in both the anti-proliferative effects of LPS and the up-regulation of P2X4 receptors. Brief incubations with phorbol esters produced a similar up-regulation of surface P2X4 receptors in bone marrow derived macrophages (BMDMs) and we are examining the underlying mechanisms involved.

Authors have confirmed where relevant, that experiments on animals and man were conducted in accordance with national and/or local ethical requirements.

PC84

Channel blocking properties of a partial agonist at the human muscle acetylcholine receptor

R. Lape, D. Colquhoun and L.G. Sivilotti

Pharmacology, UCL, London, UK

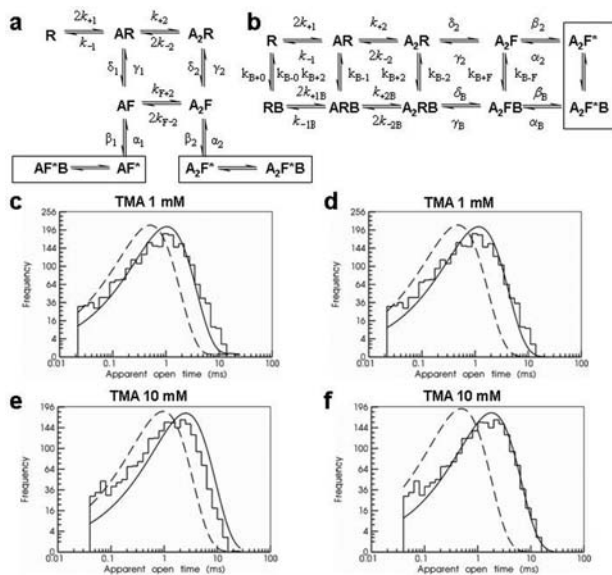
Agonists at the muscle acetylcholine receptor (AChR) can all block the channel as well as activate it. For many partial agonists e.g. choline or tetramethylammonium (TMA), concentrations for activation and block are similar.

We recorded cell-attached TMA-activated single-channel currents from HEK293 cells transfected with human nicotinic AChRs ($\alpha\beta\delta\epsilon$, transfection ratio 2:1:1:1). In single-channel records at -80 mV, the amplitude of the openings appears to decrease progressively with agonist concentration because of fast channel block.

Several records obtained at different TMA concentrations were fitted simultaneously with HJCFIT¹. For TMA the equilibrium constant, K_B , for open channel block was 8.9 ± 0.6 mM, as estimated from the reduction of apparent single-channel amplitude, cf EC_{50} of 2.2 ± 0.5 mM.

If essentially no blockages are detected, the open state and the open-blocked state can be treated as a single compound open state for the purpose of analysing kinetics. Such compound states are indicated by the boxes in Fig 1a and 1b. During fitting, the exit from the compound open state in Fig 1a is given by a transition rate that is not α_2 but rather $\alpha_2/(1 + c_B)$, where $c_B = [B]/K_B$ and $[B]$ is the blocker (agonist) concentration. This reflects the fact that the compound state spends only a fraction of time $1/(1 + c_B)$ in the state from which exit can occur. Similarly, for the mechanism in Fig 1b, the transition rate for leaving the compound open state via the blocked state ($A2F^*B$) is taken not as α_B but rather $\alpha_B c_B/(1 + c_B)$, i.e. α_B is multiplied by the fraction of time which the compound open state spends in the blocked state. The left column shows a fit with a mechanism that allows block of channels only when they are open. The predicted distribution of apparent open times at the lower concentration (1 mM, Fig 1c) of TMA superimposes on the observations quite well, but at the higher concentration (10 mM, Fig 1e) the prediction is poor. The predominant mean apparent open time is about 1.5 times smaller than is predicted.

The right column in Fig 1 shows fit of a mechanism (Fig 1b) in which the block is not selective for the open state, but can occur from any state. In this case the distribution of apparent open times is predicted accurately at both low and high concentrations of TMA. The mean values were $\alpha_2 = 2370 \text{ s}^{-1} \pm 12\%$ (CVM, $n = 4$ fits) and $\alpha_B = 1550 \text{ s}^{-1} \pm 19\%$, so the channel shuts almost as fast when it is blocked as when it is not. The mean opening transition rate for the unblocked channel was $\beta_2 = 71300 \text{ s}^{-1} \pm 9\%$, similar to that for acetylcholine², and for the blocked channel, the mean opening rate was almost as fast, $\beta_B = 49000 \text{ s}^{-1} \pm 9\%$. Thus TMA seems not act as a pure open channel blocker, but AChRs blocked by TMA can close and return to their resting state without re-opening.



Colquhoun et al. (2003) *J Physiol* 547, 699-728.

Hatton et al. (2003) *J Physiol* 547, 729-760.

Funded by the Wellcome Trust and the MRC.

Authors have confirmed where relevant, that experiments on animals and man were conducted in accordance with national and/or local ethical requirements.

PC85

The Na⁺/H⁺ exchanger isoform 3 is the key proton recycling mechanism to drive PepT1-mediated dipeptide transport in native murine intestine

M. Chen¹, A. Singh¹, U. Dringenberg¹, R. Engelhardt¹, B. Riederer¹, M. Manns¹, I. Rubio², M. Soleimani³, G. Shull³, H. Daniel² and U. Seidler¹

¹Medizinische Hochschule Hannover, Hannover, Germany,

²Technical University of Munich, Weihenstephan, Germany and

³University of Cincinnati, Cincinnati, OH, USA

Background: Inhibition of the apical Na⁺/H⁺ exchanger isoform 3 (NHE3) activity interferes with dipeptide uptake in intestinal cell lines. **Aim:** This study investigates how dipeptide transport affects murine jejunal fluid absorption and enterocyte pHi in vivo, whether NHE3 function is mandatory for PepT1 function in the native intestine, and whether the reason for its importance lies in its ability to regulate enterocyte pHi during H⁺/dipeptide uptake. **Methods and Results:** The luminal application of Gly-Sar resulted in a strong, PepT1- as well as NHE3-dependent increase in intestinal fluid secretion, measured by single-pass perfusion, and a decrease in villous enterocyte pHi, measured by two-photon microscopy in the anesthetized mouse (administration of 10 µL/g intraperitoneal (IP) haloperidol/midazolam/fentanyl cocktail (haloperidol 12.5 mg/Kg, fentanyl 0.325 mg/Kg and midazolam 5 mg/Kg body weight)). It also caused a strong short circuit current (Isc) response in chambered jejunal mucosa in vitro, which was not influenced by the

absence or presence of the luminal Cl⁻/HCO₃⁻ exchanger SLC26a6, was absent in the absence of PepT1 expression, and was virtually abolished in the absence of NHE3 expression. Villous enterocyte pHi decreased significantly stronger upon the luminal application of Gly-Sar in the absence of SLC26a6, as well as in the absence of NHE3. The absence or inhibition of NHE1 and NHE2, which are also expressed in murine jejunum, did not affect the Gly-Sar mediated pHi-decrease. **Conclusions:** NHE3 and SLC26a6 are equally involved in pHi regulation after PepT1-mediated uptake of H⁺/dipeptide over the apical BBM, but only NHE3 is essential for both PepT1-mediated dipeptide as well as salt and fluid absorption. The requirement of NHE3 for PepT1-mediated transport may be explained by a unique H⁺-recycling function of NHE3 in conjunction with PepT1.

Authors have confirmed where relevant, that experiments on animals and man were conducted in accordance with national and/or local ethical requirements.

PC86

Effects of phenylephrine on spontaneous electrical waveforms in the guinea-pig prostate

D.T. Nguyen¹, R.J. Lang² and B. Exintaris¹

¹Pharmaceutical Biology, Monash University, Parkville, VIC, Australia

and ²Physiology, Monash University, Clayton, VIC, Australia

Introduction: Two distinct types of spontaneous electrical activity can be recorded from the guinea-pig prostate, slow waves and pacemaker potentials. Slow waves arise from smooth muscle cells while pacemaker potentials are believed to arise from prostatic interstitial cells (PICs). These c-kit positive cells are mainly located between the glandular epithelial and smooth muscle layers of the guinea-pig prostate and provide the depolarising pulse to neighbouring smooth muscle cells to initiate slow waves.

Aim and Methods: In this study the effects of phenylephrine on the spontaneous electrical activity in the guinea-pig prostate was investigated using intracellular microelectrodes to record changes in membrane potentials. Paired Student's t-test was used for tests of significance, values are expressed as mean ± SEM and p<0.05 was considered to be significant.

Results: Phenylephrine (1 µM) increased the frequency of slow wave activity from 3.9 ± 0.9 min⁻¹ to 9.4 ± 2.2 min⁻¹ (n=6, p<0.05) and pacemaker activity from 6.8 ± 1.0 min⁻¹ to 9.0 ± 0.9 min⁻¹ (n=3, p<0.05) without affecting other measured parameters. In the presence of nifedipine (1 µM), phenylephrine also increased the frequency of both waveforms and in addition caused a membrane depolarisation from -53.4 ± 1.7 mV to -51.0 ± 1.9 mV in slow waves (n=8, p<0.05) and -51.4 ± 2.8 mV to -47.6 ± 2.5 mV in pacemaker potentials (n=3, p<0.05). In cells where nifedipine abolished the spontaneous electrical activity, phenylephrine was able to restore activity which was associated with a resting membrane depolarisation of 2-4 mV (n=7, p<0.05). In the presence of nifedipine, cyclopiazonic acid (CPA, 10 µM), carbonyl cyanide 3-chlorophenylhydrazone (CCCP, 1-10 µM) or niflumic acid (10-100 µM) abolished electrical activity. In the presence of CPA or CCCP, phenylephrine

further depolarised the membrane potential by 6mV (n=5, p<0.05) and 4mV (n=5, p<0.05), respectively, however, was unable to restore the abolished electrical activity. Phenylephrine restored the electrical activity blocked by niflumic acid, with most measured parameters comparable to those in nifedipine alone.

Conclusion: Altogether, these results suggest that the increased slow wave frequency observed by the addition of phenylephrine is likely due to its effects on PICs as phenylephrine increased the frequency of both pacemaker potentials and slow waves. The effects of phenylephrine were dependent upon Ca^{2+} cycling by internal Ca^{2+} stores within the endoplasmic reticulum and mitochondria, but not by the activation of Cl^- channels.

Authors have confirmed where relevant, that experiments on animals and man were conducted in accordance with national and/or local ethical requirements.

PC86A

erg current in mouse gonadotropes

C.E. Dinu¹, J.R. Schwarz¹, W. Hirdes¹, S. Wen¹, D. Niculescu¹, C.K. Bauer² and U. Boehm¹

¹Institut für Neurale Signalverarbeitung, Zentrum für Molekulare Neurobiologie Hamburg, Hamburg, Germany and ²Institute for Vegetative Physiology and Pathophysiology, University Hospital Hamburg-Eppendorf, Hamburg, Germany

Srinivas S, Watanabe T, Lin CS, William CM, Tanabe Y, Jessell TM, Costantini F (2001). BMC Dev Biol 1:4

Bauer CK, Schwarz JR (2001). J Membrane Biol 182: 1-15

Eggen K, Baldwin K, Tackett M, Osborne J, Gogos J, Chess A, Axel R, Jaenisch R (2004). Nature 428: 44-9

Hille B, Tse A, Tse FW, Bosma M (1995). Recent Progress in Hormone Research 50: 75-95

Stojilkovic S, Zemkova H, Van Goor F (2005). Trends in Endocrinology and Metabolism 16: 152-159

Authors have confirmed where relevant, that experiments on animals and man were conducted in accordance with national and/or local ethical requirements.

PC87

Reversible disruption of AE2 expression at the rat blood-brain barrier following transient focal astrocyte loss

S. Wang¹, C.L. Willis², S.B. Hladky¹ and M.A. Barrand¹

¹Pharmacology, University of Cambridge, Cambridge, Cambridgeshire, UK and ²Medical Pharmacology, University of Arizona, Tucson, AZ, USA

The endothelial cells of the blood-brain barrier secrete HCO_3^- ions into the brain. On the present evidence it is likely that the

normal secretion occurs via Na^+ -driven HCO_3^- transport into the endothelial cells together with efflux via $\text{Cl}^-/\text{HCO}_3^-$ exchange [1]. The leading candidate for the efflux transporter is AE2 as mRNA for AE2 is prominently expressed in the primary cultured endothelial cells and AE2 protein is associated with the microvessels in brain slices and is seen in Western blots from the cultured cells [2]. It is well documented that astrocytes are involved in induction and maintenance of various blood-brain barrier features but there are few reports on their influence on ion transporters.

We here report an investigation on the effects of astrocytes on endothelial cells employing a method of selective ablation of astrocytes in the brain [3]. This method uses systemic injection of 3-chloropropanediol which produces focal loss of GFAP positive astrocytes in certain brain regions including the inferior colliculus. In this region there was virtually complete loss of GFAP expressing astrocytes from 3 to 6 days after injection. There were marked changes in expression of occludin and claudin 5 from PECAM-1 expressing microvessels over a similar time course and these were reversed soon after repopulation of the region with astrocytes. P-glycoprotein expression also markedly decreased and recovered with a similar time course [4]. The present study follows changes in expression of AE2 protein in microvessels using the same methods.

AE2 and the endothelial cell marker PECAM-1 were visualized on microvessels in frozen rat brain sections using fluorescence microscopy. This method included antigen unmasking with 1% SDS [5] as reported previously [2]. PECAM-1 remained clearly expressed throughout the next 28 days, but the distribution of AE2 first became discontinuous and then largely disappeared over 3 days. Recovery was underway at 14 days and appeared to return to normal levels by 28 days coincident with the reappearance of GFAP immunoreactive astrocytes. These in vivo results suggest that with AE2, as with P-glycoprotein, there may be a substantial decrease in expression in brain endothelial cells once these cells are removed from the influence of astrocytes and grown in culture. Hence the previously reported transport rates of HCO_3^- in cultured cells may have underestimated the transport rates occurring in vivo.

Nicola PA et al (2008) Pflugers Arch. DOI 10.1007/s00424-007-0441-x.

Wang S et al Proceedings Life Sciences. The Physiological Society: Glasgow 2007:PC54.

Willis CL et al (2004) Glia 48:1-13.

Willis CL et al (2007) Brain Res. 1173:126-136.

Brown, D. et al (1996) Histochem. Cell Biol. 105(4): 261-267.

The SA6 antibody for AE2 was kindly provided by Dr. Seth Alper, Beth Israel Deaconess Medical Center, 330 Brookline Avenue, Boston. This work was supported by a grant from the BBSRC. SW held a Cambridge Overseas Trust Scholarship.

Authors have confirmed where relevant, that experiments on animals and man were conducted in accordance with national and/or local ethical requirements.